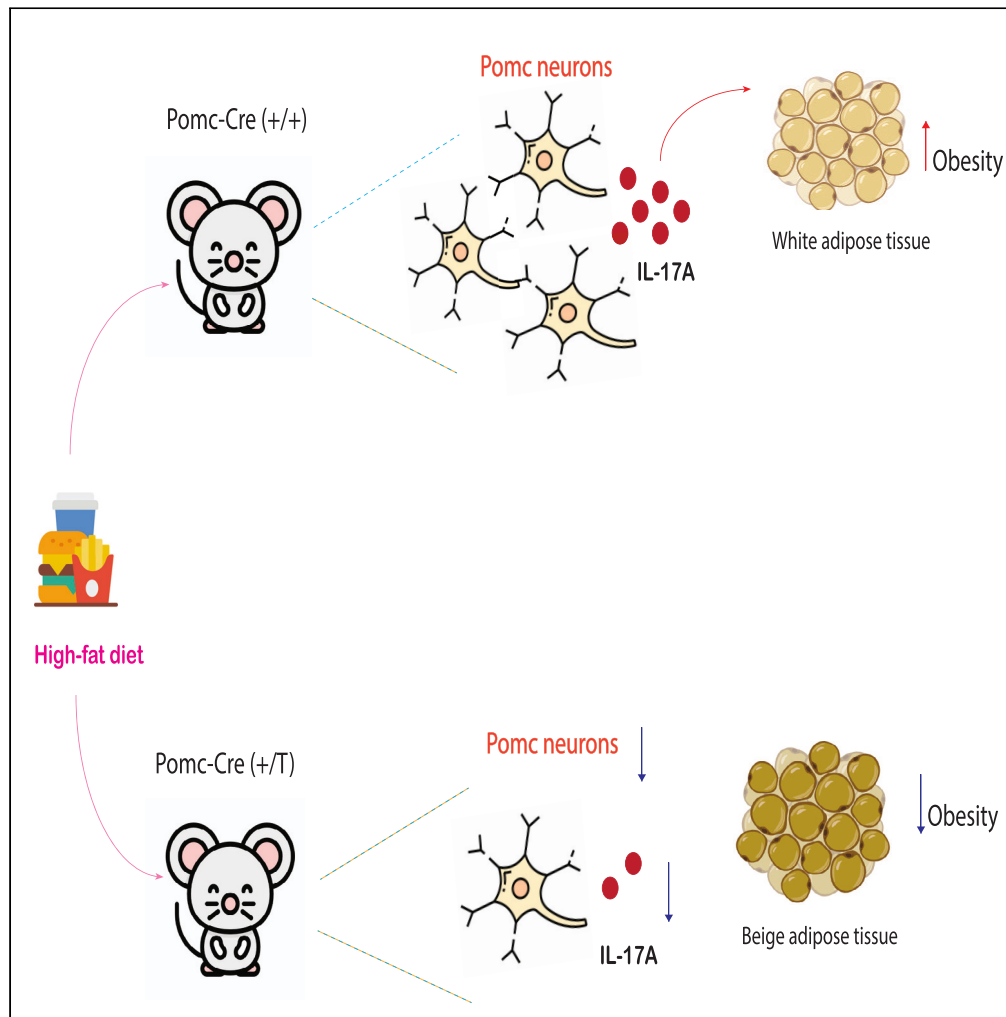**Article**

IL-17A produced by POMC neurons regulates diet-induced obesity

Rosa Gallo, Ana Teijeiro, Mariana Angulo-Aguado, Nabil Djouder

ndjouder@cnio.es

Highlights

Pomc-Cre mouse causes unintended weight loss

POMC neurons produce IL-17A upon high-fat diet

Pomc-Cre mouse has reduced levels of POMC neurons and IL-17A affecting body weight

Article

IL-17A produced by POMC neurons regulates diet-induced obesity

Rosa Gallo,[1,2] Ana Teijeiro,[1,2] Mariana Angulo-Aguado,[1,2] and Nabil Djouder[1,3,*]

SUMMARY

Overeating leads to obesity, a low-grade inflammatory condition involving interleukin-17A (IL-17A). While pro-opiomelanocortin (POMC) neurons regulate feeding, their connection with IL-17A is not well understood. To impair IL-17A signaling in POMC neurons, IL-17A receptor (*Il17ra*) was deleted by crossing *IL17ra*-flox and *Pomc-Cre* mice. Despite effective deletion, these mice showed no differences in body weight or adiposity compared to control mice, challenging the idea that IL-17A induces obesity through POMC neuron regulation. However, both groups exhibited reduced weight gain and adiposity upon high-fat diet compared to mice carrying only the floxed alleles, suggesting independent effects of *Pomc-Cre* transgene on body weight. Further analysis reveals that POMC neurons express IL-17A, and reduction in number of POMC neurons in *Pomc-Cre* mice could be linked to decreased IL-17A expression, which correlates with reduced adipocyte gene expression associated with obesity. Our data underscore an unexpected crosstalk between IL-17A-producing POMC neurons and the endocrine system in obesity regulation.

INTRODUCTION

Nutrient overload can lead to obesity, a low-grade inflammatory disease.[1] In mammals, feeding behavior is regulated by neurons that express pro-opiomelanocortin (POMC) or agouti-related protein (AgRP) in the arcuate nucleus (ARC) region of the hypothalamus. Whereas AgRP neurons enhance food intake,[2] POMC neurons play a critical role in the regulation of body weight and energy balance through the production of alpha-melanocyte-stimulating hormone (α-MSH) that can act as an appetite suppressant by binding to and activating the melanocortin receptors in the brain.[3–5] In obese individuals, there is often a reduction in POMC expression, leading to decreased α-MSH production and increased appetite.[6,7] Additionally, genetic mutations in the *POMC* gene have been linked to early-onset obesity in humans.[8,9] Leptin, a hormone produced by adipocytes and increased in obese individuals also contributes to the activation of POMC neurons.[10] Therefore, dysregulation of POMC neurons plays a critical role in the onset of obesity by increasing food intake.

The pro-inflammatory cytokine interleukin-17A (IL-17A) is produced by innate and adaptive lymphocytes, plays fundamental functions in tissue physiology and influences a wide range of biological processes beyond host defense, such as neural repair or adipocyte metabolism.[1,11] Not only have increases in circulating IL-17A levels been observed after feeding in mice and humans,[11,12] it also exerts a direct influence on adipocytes, triggering metabolic reprogramming that fosters diet-induced obesity (DIO) and contributes to the development of metabolic syndrome, without affecting food intake.[1] Interestingly, systemic administration of IL-17A causes a temporal increase in both POMC and AgRP expression.[11,12] Accordingly, hypothalamic astrocytes and microglia express IL-17RA,[11,13] suggesting a broader role of IL-17A in hypothalamus. Additionally, IL-17A has been reported to play a role in the regeneration of sensory neurons.[14] While a distinct role of IL-17A in adipocyte reprogramming has been proposed to be crucial for obesity, these findings suggest that IL-17A may promote obesity through the modulation of POMC neurons, linking brain to adipocyte biology.

The *Cre*-lox system has proven to be a valuable tool in studying the role of arcuate neurons in the regulation of feeding and energy expenditure in mice. The *Pomc-Cre* mouse that expresses the *Cre* recombinase enzyme under the control of the *Pomc* promoter has been widely used in research to study the function of POMC neurons *in vivo*.[15–18] By using the *Pomc-Cre* mouse line in combination with mice that carry loxP-flanked genes, researchers can selectively delete or modify genes specifically in POMC neurons, allowing them to investigate the role of these genes in physiology. For instance, the *Pomc-Cre* has been used to study the function of melanocortin pathway in the regulation of body weight.[16] It has also been utilized to understand how melanocortin neurons integrate endocrine signals to protect female mice against DIO.[18] Additionally, deleting the regulatory molecule miR-29a in the *Pomc-Cre* mouse has been shown to attenuate obesity in adult mice fed with high-fat diet (HFD).[17] Therefore, studies using *Pomc-Cre* mouse models have provided valuable insights into the functions of POMC neurons

[1]Growth Factors, Nutrients and Cancer Group, Molecular Oncology Programme, Centro Nacional de Investigaciones Oncológicas, CNIO, 28029 Madrid, Spain
[2]These authors contributed equally
[3]Lead contact
*Correspondence: ndjouder@cnio.es
https://doi.org/10.1016/j.isci.2024.110259

in the regulation of appetite and energy balance and have helped to identify potential therapeutic targets for obesity and related metabolic disorders.

Here, we sought to investigate the role of IL-17A in modulating POMC neurons and its effect on obesity. To this end, we deleted IL-17A receptor (IL-17RA) specifically in POMC neurons and analyzed the effects on body weight, comparing the results with the *Pomc-Cre* line mouse. Our study demonstrates off-target effects induced by the *Pomc-Cre* transgene, which may contribute to physiological and metabolic phenotypes that are inherent to the *Cre-lox* system rather than the result of the deletion of the genes of interest in the POMC neurons. Precisely, we demonstrate that POMC neurons express IL-17A during DIO and this could be implicated in the off-target effects elicited by the *Pomc-Cre* line.

RESULTS

Deletion of IL-17RA in POMC neurons does not affect mouse body weight

To elucidate the function of IL-17A signaling in POMC neurons, IL-17RA was deleted in these neurons by crossing *IL17ra*-flox mice[19] (hereafter *Il17ra*(flox-flox) mice) with *Pomc-Cre* mice[15] (hereafter *Il17ra*(+/+)Pomc mice) in order to produce *Il17ra*(Δ/Δ)Pomc mice. Adult mice were fed for 2 months with HFD (Figure 1A). Co-immunofluorescence (CIF) and bioinformatics analysis from published datasets[2,20] confirmed that IL-17RA is abundantly expressed in POMC neurons in the ARC region of the hypothalamus, and this expression is efficiently abolished when IL-17RA is genetically depleted (Figures 1B, S1A, and S1B). Notably, *Il17ra*(Δ/Δ)Pomc mice with ablation of *Il17ra* in POMC neurons had similar body weight (Figures 1C–1F) and adiposity (Figures 1G–1I) to *Il17ra*(+/+)Pomc littermate controls, suggesting that IL-17A does not act on POMC neurons to induce obesity. However, upon HFD treatment, both cohorts of mice expressing the *Pomc-Cre* mouse gained less weight and had less adiposity than *Il17ra*(flox-flox) littermates (Figures 1G–1I). Notably, *Il17ra*(Δ/Δ)Pomc mice and *Il17ra*(+/+)Pomc control littermates fed with normal diet (ND) showed similar body weight and adiposity (Figures 1C–1F). These data strongly points out that the *Pomc-Cre* strain has an effect on body weight following HFD that is independent on the absence of *Il17ra* in POMC neurons. Therefore, IL-17A regulates adipocyte biology independently of POMC neurons or food intake to promote obesity, as previously shown.[1]
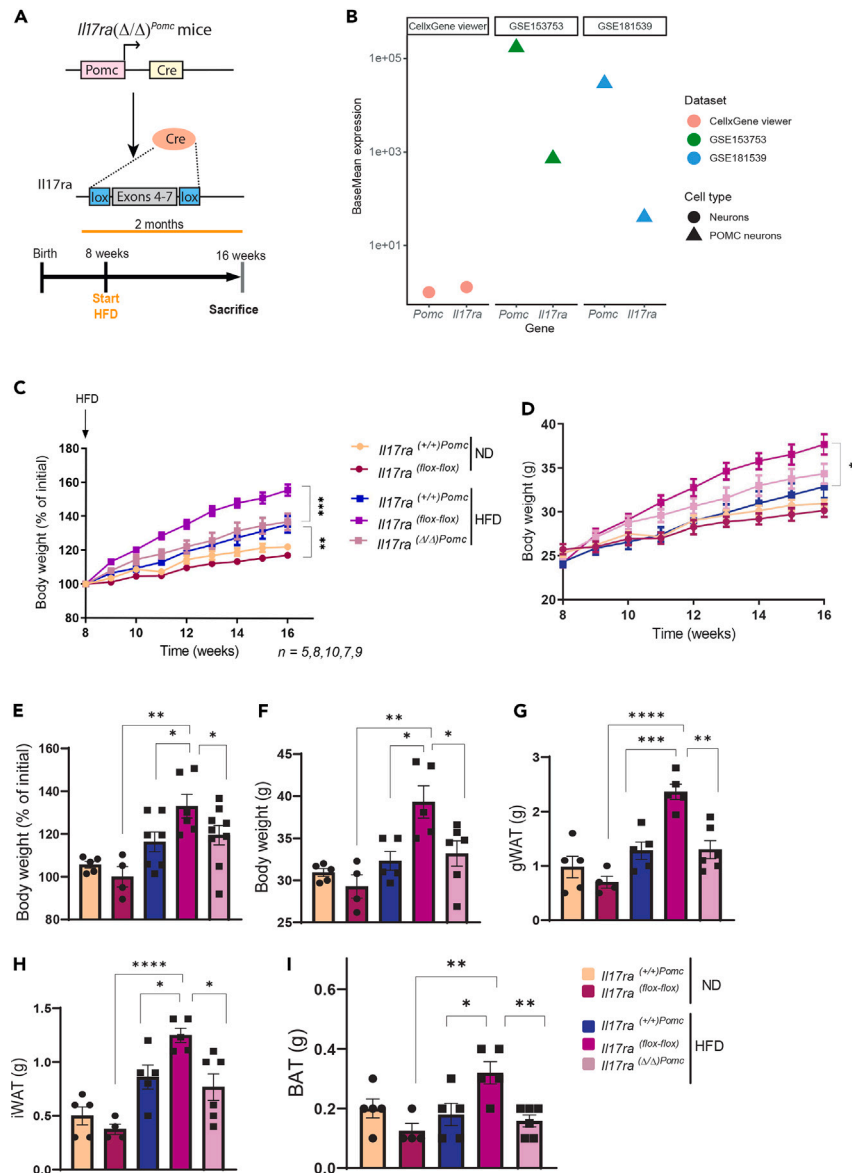
Deletion of SOCS3 in POMC neurons does not affect mouse body weight

To confirm the off target-effects of the *Pomc-Cre* mouse, we sought investigating the role of the suppressor of cytokine signaling 3 (*Socs3*) in modulating obesity via regulation of POMC neurons. SOCS3 acts as a negative regulator of cytokine signaling, inhibiting the activation of JAK/STAT signaling pathway, resulting in gene expression changes.[21–23] Mice with neural cell-specific *Socs3* deletion display increased insulin sensitivity and are protected against DIO,[24] whereas overexpression of *Socs3* has the opposite effect.[25] Notably, Wang et al. and Kievit et al. published important findings indicating that the obesogenic effects of *Socs3* and associated metabolic dysfunctions are mediated through the regulation of the POMC neurons in the hypothalamus.[26,27] Depletion of SOCS3 specifically in murine POMC neurons protects against metabolic dysfunctions and DIO.[24,26,27] However, noteworthy authors did not use *Pomc-Cre* littermate controls to compare the obtained data, which is especially important because during development, POMC is transiently and broadly expressed in various neurons of the central nervous system that differ from POMC neurons in adulthood.[28] Therefore, to check whether *Pomc-Cre* transgene is indeed generating effects on body weight loss, as demonstrated for IL-17RA deletion, we conducted a crossbreeding experiment between *Pomc-Cre*[15] mice (hereafter *Socs3*+/+(Pomc) mice) with *Socs3*-flox[29] (hereafter *Socs3*(flox-flox) mice) mice, which resulted in the generation of *Socs3*(Δ/Δ)Pomc mice with specific deletion of *Socs3* in POMC neurons (Figure 2A). IF analysis indicated that *Socs3* was efficiently deleted in POMC neurons (Figures S2A and S2B). However, in contrast to the findings reported by Wang et al. and Kievit et al.,[26,27] our results indicate that *Socs3*(Δ/Δ)Pomc mice fed with HFD had similar body weights (Figures 2B–2E) and adiposity (Figures 2F–2H) to those of the *Socs3*(+/+)Pomc wild-type littermates. Importantly, *Socs3*(flox-flox) mice upon HFD gained more weight (Figures 2B–2E) and had more adiposity than the littermates that had the *Pomc-Cre* line (*Socs3*(+/+)Pomc) (Figures 2F–2H). Notably, *Socs3*(flox-flox) mice and *Socs3*(+/+)Pomc wild-type littermates (*Pomc-Cre* line) had similar body weight without any effects on adiposity upon ND (Figures 2B–2H). These results confirm that increased body weight observed upon HFD is primarily caused by the transgenic *Pomc-Cre* gene rather than the ablation of *Socs3,* as also shown for IL-17RA depletion.

POMC neurons express IL-17A upon HFD

Next, we investigated the mechanisms through which the transgenic *Pomc-Cre* mouse model gained less body weight when fed with HFD. Notably, there was an evident decrease in the number of neurons expressing POMC in the ARC region of the hypothalamus, in *Pomc-Cre* mice compared to the wild-type littermate control (Figures 3A and 3B). Reverse transcription-quantitative polymerase chain reaction (RT-qPCR) confirmed a decrease in *Pomc* levels without any significant effects on *Socs3* mRNA levels in the hypothalamus of the *Pomc*-Cre mice (Figures 3C and 3D), suggesting the decrease in POMC neurons. Remarkably, it became evident that *Pomc-Cre* mice also exhibited reduced IL-17A levels (Figure 3E), suggesting that the insertion of the transgene could affect IL-17A expression. Accordingly, bioinformatics analysis conducted on various publicly available datasets highlighted that POMC neurons expressed *IL17a* and *Rorc*, a well-known transcription factor associated with IL-17A (Figure 3F).[1] Co-IF confirmed that IL-17A is highly expressed in POMC neurons, and its expression is significantly reduced in the ARC region of the hypothalamus of the *Pomc-Cre* mice compared to the wild-type littermates (Figures 3A and 3G).

Considering the pivotal role of IL-17A in mediating obesity through adipocyte reprogramming and phosphorylation of PPARγ, the observed phenotype in *Pomc-Cre* mice could potentially find its explanation in the diminished POMC neurons and reduced IL-17A levels. As a result of this, the white adipose tissue of *Pomc-Cre* mice had decreased expression of phosphorylated PPARγ-targeted genes associated

Figure 1. Deletion of IL-17RA in POMC neurons does not affect mouse body weight

(A) Representation of the construct to generate $Il17ra^{(\Delta/\Delta)Pomc}$ mice. Below is the scheme of HFD treatment in $Il17ra^{(\Delta/\Delta)Pomc}$ mice from 8 weeks to 16 weeks.

(B) Base mean expression profiles of POMC and IL-17RA in neurons (denoted as dots) and POMC-expressing neurons (denoted as triangles).

(C) Weights of mice fed with HFD or ND beginning at 8 weeks normalized to the initial body weight (n = 5, 8, 10, 7, 9 mice; $Il17ra^{(flox-flox)}$ upon ND versus $Il17ra^{(flox-flox)}$ upon HFD; $p=0.0008$; $Il17ra^{(flox-flox)}$ versus $Il17ra^{(\Delta/\Delta)Pomc}$ upon HFD; $p=0.0004$).

(D) Weights of mice fed with HFD or ND beginning at 8 weeks in grams ($Il17ra^{(flox-flox)}$ HFD-fed versus $Il17ra^{(+/+)Pomc}$ HFD-fed $p= 0.0162$).

(E) Percentage of body weights of HFD- and ND-fed mice at 16 weeks ($Il17ra^{(flox-flox)}$ upon ND versus $Il17ra^{(flox-flox)}$ upon HFD $p=0.030$; $Il17ra^{(flox-flox)}$ versus $Il17ra^{(+/+)Pomc}$ upon HFD $p=0.0400$; $Il17ra^{(flox-flox)}$ versus $Il17ra^{(\Delta/\Delta)Pomc}$ upon HFD $p=0.0270$).

(F) Body weights of HFD- and ND-fed mice at 16 weeks in grams ($Il17ra^{(flox-flox)}$ upon ND versus $Il17ra^{(flox-flox)}$ upon HFD $p=0.030$; $Il17ra^{(flox-flox)}$ versus $Il17ra^{(+/+)Pomc}$ upon HFD $p=0.0400$; $Il17ra^{(flox-flox)}$ versus $Il17ra^{(\Delta/\Delta)Pomc}$ upon HFD; $p=0.0271$).

(G) Weight of gonadal white adipose tissue (gWAT) in grams ($Il17ra^{(flox-flox)}$ upon ND versus $Il17ra^{(flox-flox)}$ upon HFD $p < 0.0001$; $Il17ra^{(flox-flox)}$ versus $Il17ra^{(+/+)Pomc}$ upon HFD $p=0.0250$; $Il17ra^{(flox-flox)}$ versus $Il17ra^{(\Delta/\Delta)Pomc}$ upon HFD $p=0.0278$).

(H) Weight of inguinal WAT (iWAT) in grams ($Il17ra^{(flox-flox)}$ upon ND versus $Il17ra^{(flox-flox)}$ upon HFD $p < 0.0001$; $Il17ra^{(flox-flox)}$ versus $Il17ra^{(+/+)Pomc}$ upon HFD $p=0.0085$; $Il17ra^{(flox-flox)}$ versus $Il17ra^{(\Delta/\Delta)Pomc}$ upon HFD $p=0.0384$).

(I) Weight of brown adipose tissue (BAT) in grams ($Il17ra^{(flox-flox)}$ upon ND versus $Il17ra^{(flox-flox)}$ upon HFD $p < 0.0047$; $Il17ra^{(flox-flox)}$ versus $Il17ra^{(+/+)Pomc}$ upon HFD $p=0.0029$; $Il17ra^{(flox-flox)}$ versus $Il17ra^{(\Delta/\Delta)Pomc}$ upon HFD $p=0.031$). p values were calculated by two-way ANOVA with repeated measures (C and D) or two-tailed Student's t test (E-I).
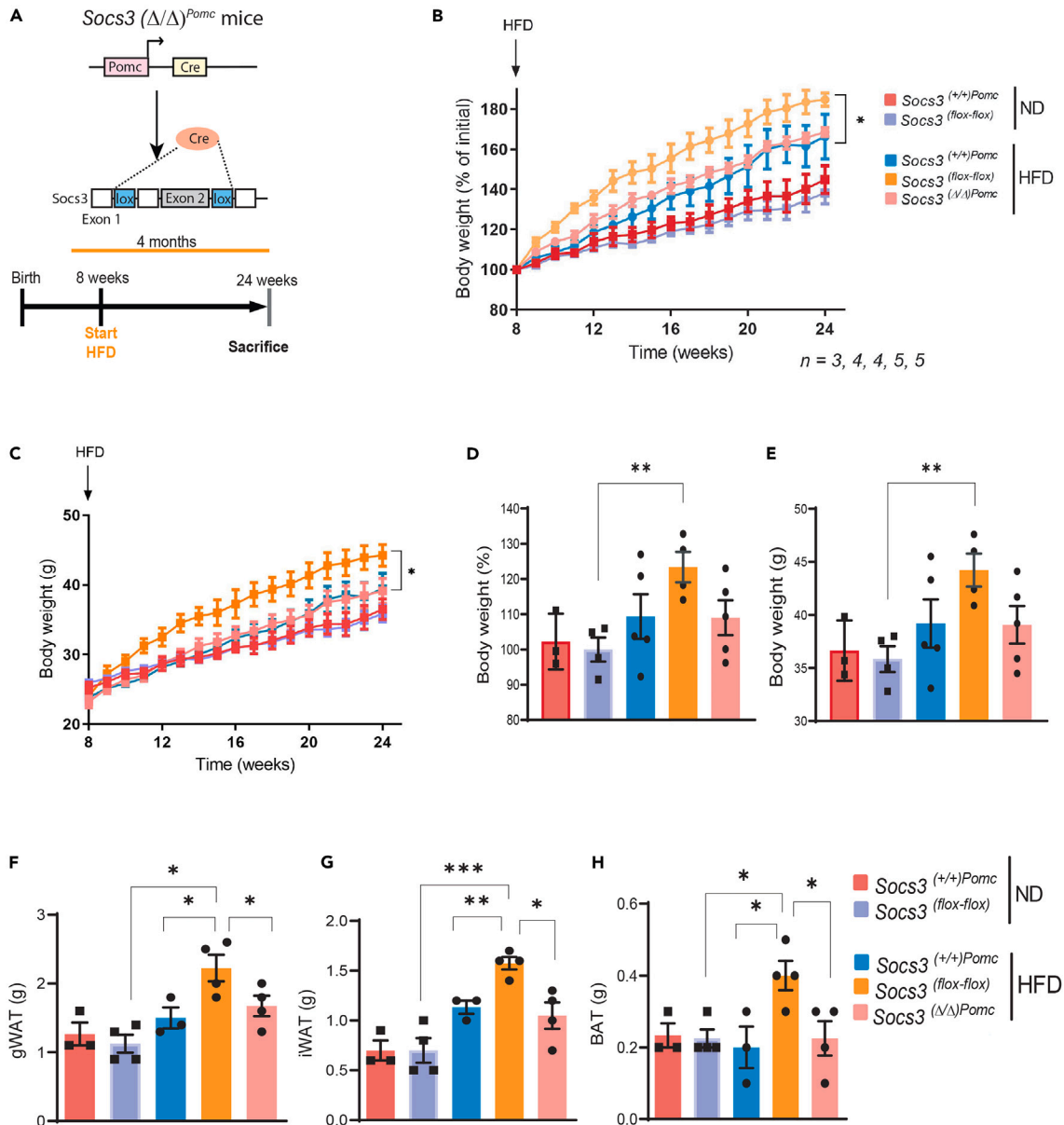
Figure 2. Deletion of SOCS3 in POMC neurons does not affect mouse body weight

(A) Representation of $Socs3^{(\Delta/\Delta)\ Pomc}$ mouse model and scheme of HFD treatment from 8 weeks to 24 weeks.

(B) Body weights of mice fed with HFD or ND beginning at 8 weeks normalized to the initial body weight. (n = 3, 4, 4, 5, 5; $Socs3^{(flox-flox)}$ HFD-fed versus $Socs3^{(+/+)Pomc}$ HFD-fed; $p=0.0224$).

(C) Body weights of mice fed with HFD or ND beginning at 8 weeks in grams ($Socs3^{(flox-flox)}$ HFD-fed versus $Socs3^{(+/+)Pomc}$ HFD-fed; $p=0.0403$).

(D) Percentage of body weights of HFD- and ND-fed mice at 24 weeks ($Socs3^{(flox-flox)}$ ND-fed versus $Socs3^{(flox-flox)}$ HFD-fed; $p=0.0054$).

(E) Body weights in grams of HFD and ND-fed mice at 24 weeks ($Socs3^{(flox-flox)}$ ND-fed versus $Socs3^{(flox-flox)}$ HFD-fed; $p=0.0054$).

(F) Weight of gonadal white adipose tissue (gWAT) in grams ($Socs3^{(flox-flox)}$ ND-fed versus $Socs3^{(flox-flox)}$ HFD-fed $p= 0.0033$; $Socs3^{(+/+)Pomc}$ HFD-fed versus $Socs3^{(flox-flox)}$ HFD-fed $p=00394$; $Socs3^{(\Delta/\Delta)Pomc}$ versus $Socs3^{(flox-flox)}$ HFD-fed $p=0.0293$)).

(G) Weight of inguinal WAT (iWAT) in grams ($Socs3^{(flox-flox)}$ ND-fed versus $Socs3^{(flox-flox)}$ HFD-fed $p= 0.0007$; $Socs3^{(+/+)Pomc}$ HFD-fed versus $Socs3^{(flox-flox)}$ HFD-fed $p=0.0051$; $Socs3^{(\Delta/\Delta)Pomc}$ versus $Socs3^{(flox-flox)}$ HFD-fed $p=0.0116$).

(H) Weight of brown adipose tissue (BAT) in grams ($Socs3^{(flox-flox)}$ upon ND versus $Socs3^{(flox-flox)}$ upon HFD; $p=0.0106$; $Socs3^{(+/+)Pomc}$ HFD-fed versus $Socs3^{(flox-flox)}$ HFD-fed $p=0.00327$; $Socs3^{(\Delta/\Delta)Pomc}$ versus $Socs3^{(flox-flox)}$ HFD-fed $p=0.0319$). p values were calculated by two-way ANOVA with repeated measures (B and C) or two-tailed Student's t test (D-H).
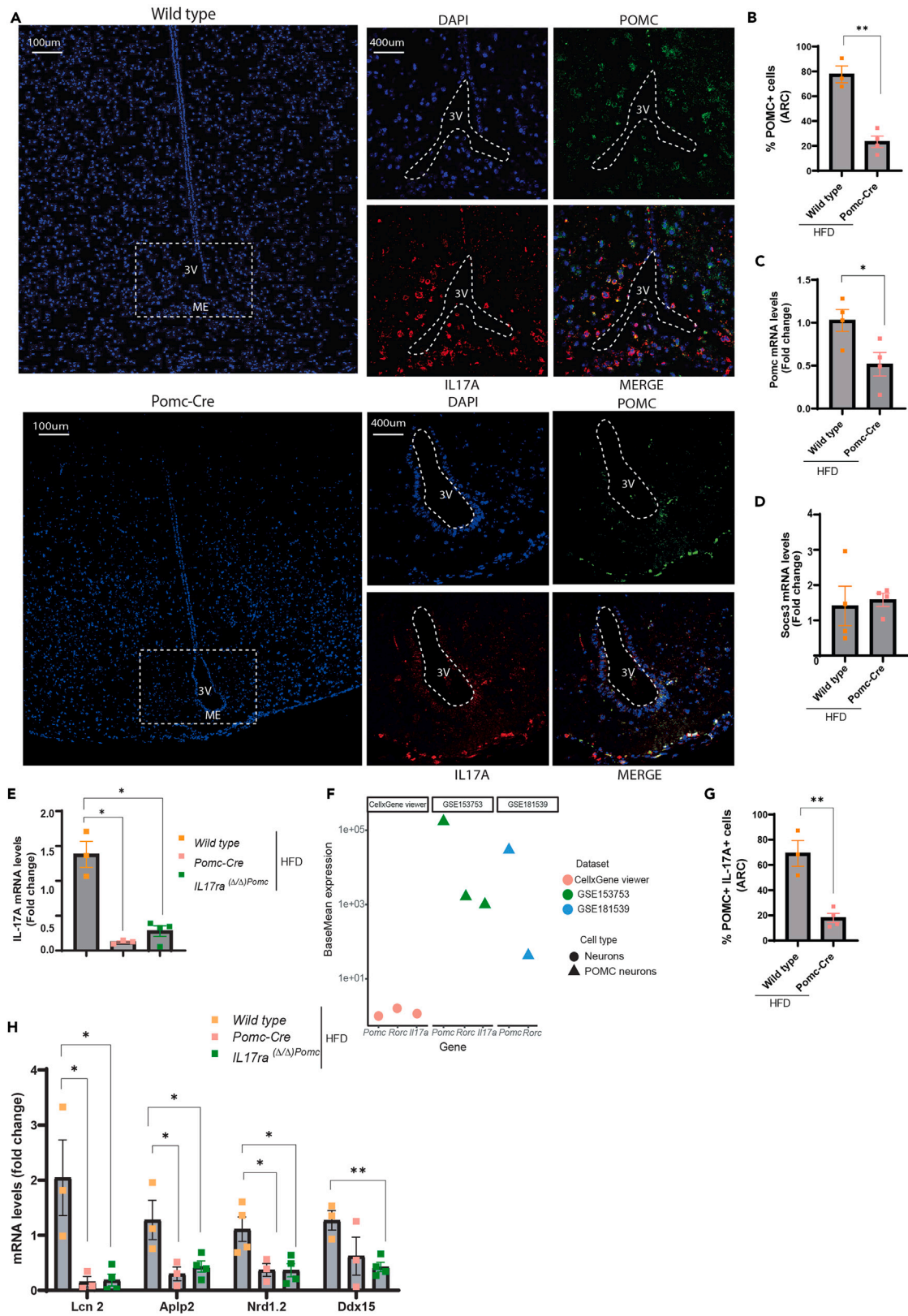
Figure 3. POMC neurons express IL-17A upon HFD

(A) Confocal images of immunofluorescence of POMC and IL-17A in arcuate nucleus (ARC) region of the hypothalamus. The right scale bar image is 100 μm, and the left scale bar image is 400 μm.

(B) Quantification of POMC positive cells in the ARC in *wild type* and *Pomc-Cre* mice fed with HFD of Figure 3A (n = 3,4; p=0.0043).

(C) Expression of *Pomc* by RT-qPCR in the brain of *Pomc-Cre* mice and wild type mice fed with HFD (n = 4,4; p=0.0342).

(D) Expression of Socs3 by RT-qPCR in the brain of *Pomc-Cre* mice and wild type mice fed with HFD (n = 4,4; p=0.7761).

(E) Expression of IL-17A measured by RT-qPCR in gonadal adipose tissue of mice fed with HFD (n = 3,3,4; *wild type* versus *Pomc-Cre* p= 0.025; *wild type* versus *Il17ra*$^{(\Delta/\Delta)Pomc}$ p= 0.017).

(F) Base mean expression profile of *Pomc*, *Rorc* and *Il17a* in neurons (denoted as dots) from https://cellxgene.cziscience.com/. and POMC-expressing neurons (denoted as triangles) from GSE153753 and GSE181539.

(G) Quantification of POMC and IL-17A positive cells in the ARC in *wild type* and *Pomc-Cre* mice fed with HFD of (A) (n = 3,4; p=0.0014).

(H) mRNA levels of IL-17A target genes in gonadal adipose tissue of *wild type*, *Pomc-Cre* and *Il17ra*$^{(\Delta/\Delta)Pomc}$ mice upon HFD. Lipocalin 2 (*Lcn2*) (*wild type* versus *Pomc-Cre* p value 0.050; *wild type* versus *Il17ra*$^{(\Delta/\Delta)Pomc}$ p value= 0.0252). Apolipoprotein 2 (*Aplp2*) (*wild type* versus *Pomc-Cre* p value 0.0473; *wild type* versus *Il17ra*$^{(\Delta/\Delta)Pomc}$ p value= 0.0338; Nuclear Receptor Subfamily 1 Group D Member 2 (*Nr1d2*) (*wild type* versus *Pomc-Cre* p value 0.0460; *wild type* versus *Il17ra*$^{(\Delta/\Delta)Pomc}$ p value= 0.0257); DEAD-Box Helicase 17 (*Ddx17*) (*wild type* versus *Pomc-Cre* p value 0.1697; *wild type*$^{)}$ versus *Il17ra*$^{(\Delta/\Delta)Pomc}$ p value= 0.0054). p value was calculated with two-tailed Student's *t* test. Every dot in the graphs represents a mouse.

with obesity (Figure 3H). Hence, POMC neurons could secrete IL-17A, which may assume a pivotal role in adipocyte biology, as previously shown,[1] operating independently of its impact on POMC neurons. Any genetic disruptions resulting in reduction of IL-17A levels could potentially result in bight loss, irrespective of food intake.

DISCUSSION

This study explores the interplay between IL-17A signaling, POMC neurons, and obesity. The anorexigenic axis mediated by POMC neurons plays a crucial role in regulating food intake and energy expenditure, and its dysregulation can lead to obesity and metabolic disorders. Here we demonstrate that IL-17RA deletion in POMC neurons using the *Pomc-Cre* transgenic mouse model does not affect body weight. The mechanistic insights into how the transgenic *Pomc-Cre* mouse could result in reduced body weight still require detailed resolution. However, our data demonstrate that POMC neurons unexpectedly could express IL-17A, the levels of which are diminished in the *Pomc-Cre* mice. There is a speculative possibility that this decrease might arise from the reduced number of POMC neurons with a reduction in POMC expression, potentially stemming from unknown mechanisms in response to variable integration of transgenic *Pomc-Cre* copies into the mouse genome.

The diminished count of POMC neurons might unlikely be the direct cause of reduced body weight gain. Accordingly, alterations in POMC neurons carrying the Cre would more likely result in increased food intake and obesity rather than satiety. However, the reduction in POMC neurons in the ARC of the hypothalamus leads to subsequent decreases in IL-17A levels, as POMC neurons can be a source of IL-17A production. The reduction in IL-17A signaling might thus contribute to body weight loss, as IL-17A is known to promote obesity through metabolic reprogramming of adipocytes,[1] rather than by regulating food intake via actions on POMC neurons. It is thus likely that the levels of IL-17A are systemically decreased in *Pomc-Cre* mice fed with HFD.

In agreement with this, our work provides evidence indicating that IL-17A signaling does not exert an impact on POMC neurons to modulate the obese state in mice. IL-17A could be therefore secreted by POMC neurons upon overnutrition affecting white adipose tissue biology. This highlights a potential unexpected crosstalk between the IL-17A-producing POMC neurons and the endocrine system to regulate obesity.

The overlooked possibility of non-specific Cre-related targets and the disparities observed in our study compared to previous findings could be also attributed to other factors.[26,27] One potential factor is the variation in the composition of the HFD used, which might influence the outcome of the studies. Similar to our study, Wang et al. used a diet with 45% fat, whereas Kievit et al. treated their mice with a diet containing a higher proportion of fat (58%).[26,27] Additionally, differences in the microbiota among the various mouse strains might play a role in influencing the outcomes. Another factor that should be taken into account is the variation in body weight between male and female mice, which can also impact the experimental results. To ensure accurate and reliable results, it is crucial to carefully address these potential confounding variables in future research. Properly controlling for diet composition, considering the impact of microbiota differences, and accounting for sex-related variations will strengthen the validity of our conclusions and enhance the translational potential of our findings.

Despite the extensive utilization of the transgenic Pomc-Cre mouse model[15] in exploring the *in vivo* functions of POMC neurons,[16–18,26,27] our study emphasizes that the mere ectopic expression of *Pomc-Cre*, irrespective of the presence of the floxed allele, induces alterations in the body weight of mice when fed an HFD. Notably, Pomc-eGFP reporter expression does not mimic the expression of tdTomato observed in the Pomc-Cre; ROSA-tdTomato mouse model, arguing that other cells than POMC neurons might be targeted by *Pomc*-Cre during embryogenesis.[28] Furthermore, it is reportedly showed that a subpopulation of cells expresses *Pomc-Cre* only during development but not in the adults.[30] Hence, it is crucial to validate the data obtained from the *Pomc-Cre* mouse model[15] by employing alternative *Pomc-Cre* mice that undergo recombination at a distinct stage of embryonic development, as indicated by previous studies.[31] Nevertheless, tracking POMC neurons across both developmental and adult stages could provide additional insights into this characteristic. On the other hand, the use of the *Cre-lox* system to delete genes of interest temporally could certainly be useful. In fact, using Tg(Pomc-Cre/ERT2) to delete serotonin receptor 2C in POMC neurons shows no significant effects on body weight when compared to their littermate controls.[32] This tamoxifen-induced CreERT2 system mainly promotes the expression of *Cre-ERT2* in adult POMC neurons, bypassing any issues encountered during embryogenesis.[10,33] However, it is important to acknowledge that tamoxifen treatments might potentially influence adult

neurogenesis. Another alternative would be the employment of the CRISPR-mediated gRNA to generate a knock-in mouse model. However, it is essential to consider that this method may also give rise to considerable off-target effects.

In sum, our work uncovers notable constraints in the transgenic *Pomc-Cre* mouse model, resulting in diminished IL-17A levels within POMC neurons and subsequently causing decreased body weight in response to DIO. Although the *Cre-lox* system is a valuable tool, it is not without its potential drawbacks. Due to the stochastic nature of DNA recombination, the efficacy of the system may be limited, and the expression of the *Cre* recombinase enzyme may cause inefficient or non-specific deletion of the gene of interest,[34,35] resulting in off-target effects that may yield unexpected results. Therefore, it is critical to use appropriate controls such as *Cre*-littermate controls (mice expressing the *Cre* enzyme) when employing the *Cre-lox* system to distinguish phenotypes triggered by the modulation of the gene of interest's expression from phenotypes linked to the Cre's insertion into the genome.

Limitations of the study

This study primarily focuses on investigating the off-target effects of the *Pomc-Cre* mouse model.[15] Our data suggest that POMC neurons can secrete IL-17A in response to HFD, and the reduction of POMC neurons in the *Pomc-Cre* mouse may contribute to lower body weight. Genetic ablation of IL-17A or RORγt in POMC neurons could serve as valuable models to demonstrate that IL-17A is secreted by these neurons and to elucidate the function of POMC IL-17A^{+} neurons in the context of the *Pomc-Cre* mouse model and in obesity. Moreover, the precise molecular mechanisms driving this phenomenon require further exploration, and it remains unclear whether systemic levels of IL-17A are decreased. We hypothesize that IL-17A's potential action may involve autocrine signaling within white adipose tissue, given that compromising IL-17A signals in this tissue has been shown to reduce body weight gain.[1] Additionally, it would be of great interest to monitor the function and activity of POMC neurons in the *Pomc-Cre* mouse through electrophysiological analysis. It is also important to acknowledge that our study is limited to one specific *Pomc-Cre* mouse model. To gain a comprehensive understanding of potential off-target effects in metabolic studies, it would be valuable to investigate other *Pomc-Cre* lines, including the *Pomc-creERT2* mouse model.[31,32] This will help determine if the observed effects are specific to the *Pomc-Cre* mouse or if they are consistent across various *Pomc-Cre* models. Furthermore, it is worth noting that our study does not exclude the possibility that the reduction of POMC neurons we observed could be due to aberrations during embryonic development. Therefore, a thorough tracking of POMC neurons throughout both the developmental and adult stages could provide valuable insights into this aspect.

STAR★METHODS

Detailed methods are provided in the online version of this paper and include the following:

- KEY RESOURCES TABLE
- RESOURCE AVAILABILITY
  - Lead contact
  - Materials availability
  - Data and code availability
- EXPERIMENTAL MODEL AND STUDY PARTICIPANT DETAILS
  - Animal models
- METHOD DETAILS
  - Mouse conditions and housing
  - Mouse diets
  - Mouse genotyping
  - Body weight
  - Tissue preparation
  - Immunofluorescence
  - Reverse transcription-quantitative polymerase chain reaction (RT-qPCR)
  - Bioinformatics analysis
- QUANTIFICATION AND STATISTICAL ANALYSIS
  - Image analysis and quantifications
  - Statistical analysis

SUPPLEMENTAL INFORMATION

Supplemental information can be found online at https://doi.org/10.1016/j.isci.2024.110259.

AUTHOR CONTRIBUTIONS

R.G., A.T., M.A.A., and N.D. designed the experiments. R.G. and A.T. performed most of the experiments and statistical analyses. M.A.A. assisted in IF workflow and analysis, performed the bioinformatics analysis and RT-qPCR. N.D. conceived the project and study and secured funding. N.D. wrote the manuscript with R.G. All authors reviewed and contributed to the editing of the manuscript.

DECLARATION OF INTERESTS

The authors declare no competing interests.

REFERENCES

1. Teijeiro, A., Garrido, A., Ferre, A., Perna, C., and Djouder, N. (2021). Inhibition of the IL-17A axis in adipocytes suppresses diet-induced obesity and metabolic disorders in mice. Nat. Metab. 3, 496–512. https://doi.org/10.1038/s42255-021-00371-1.

2. Biglari, N., Gaziano, I., Schumacher, J., Radermacher, J., Paeger, L., Klemm, P., Chen, W., Corneliussen, S., Wunderlich, C.M., Sue, M., et al. (2021). Functionally distinct POMC-expressing neuron subpopulations in hypothalamus revealed by intersectional targeting. Nat. Neurosci. 24, 913–929. https://doi.org/10.1038/s41593-021-00854-0.

3. Krashes, M.J., Lowell, B.B., and Garfield, A.S. (2016). Melanocortin-4 receptor–regulated energy homeostasis. Nat. Neurosci. 19, 206–219. https://doi.org/10.1038/nn.4202.

4. Quarta, C., Claret, M., Zeltser, L.M., Williams, K.W., Yeo, G.S.H., Tschöp, M.H., Diano, S., Brüning, J.C., and Cota, D. (2021). POMC neuronal heterogeneity in energy balance and beyond: an integrated view. Nat. Metab. 3, 299–308. https://doi.org/10.1038/s42255-021-00345-3.

5. Huszar, D., Lynch, C.A., Fairchild-Huntress, V., Dunmore, J.H., Fang, Q., Berkemeier, L.R., Gu, W., Kesterson, R.A., Boston, B.A., Cone, R.D., et al. (1997). Targeted disruption of the melanocortin-4 receptor results in obesity in mice. Cell 88, 131–141. https://doi.org/10.1016/s0092-8674(00)81865-6.

6. Cui, J., Ding, Y., Chen, S., Zhu, X., Wu, Y., Zhang, M., Zhao, Y., Li, T.R.R., Sun, L.V., Zhao, S., et al. (2016). Disruption of Gpr45 causes reduced hypothalamic POMC expression and obesity. J. Clin. Invest. 126, 3192–3206. https://doi.org/10.1172/jci85676.

7. Souza, G.F.P., Solon, C., Nascimento, L.F., De-Lima-Junior, J.C., Nogueira, G., Moura, R., Rocha, G.Z., Fioravante, M., Bobbo, V., Morari, J., et al. (2016). Defective regulation of POMC precedes hypothalamic inflammation in diet-induced obesity. Sci. Rep. 6, 29290. https://doi.org/10.1038/srep29290.

8. Farooqi, I.S., Drop, S., Clements, A., Keogh, J.M., Biernacka, J., Lowenbein, S., Challis, B.G., and O'Rahilly, S. (2006). Heterozygosity for a POMC-Null Mutation and Increased Obesity Risk in Humans. Diabetes 55, 2549–2553. https://doi.org/10.2337/db06-0214.

9. Krude, H., Biebermann, H., Luck, W., Horn, R., Brabant, G., and Grüters, A. (1998). Severe early-onset obesity, adrenal insufficiency and red hair pigmentation caused by POMC mutations in humans. Nat. Genet. 19, 155–157. https://doi.org/10.1038/509.

10. Caron, A., Dungan Lemko, H.M., Castorena, C.M., Fujikawa, T., Lee, S., Lord, C.C., Ahmed, N., Lee, C.E., Holland, W.L., Liu, C., and Elmquist, J.K. (2018). POMC neurons expressing leptin receptors coordinate metabolic responses to fasting via suppression of leptin levels. Elife 7, e33710. https://doi.org/10.7554/eLife.33710.

11. Douglas, A., Stevens, B., and Lynch, L. (2023). Interleukin-17 as a key player in neuroimmunometabolism. Nat. Metab. 5, 1088–1100. https://doi.org/10.1038/s42255-023-00846-3.

12. Nogueira, G., Solon, C., Carraro, R.S., Engel, D.F., Ramalho, A.F., Sidarta-Oliveira, D., Gaspar, R.S., Bombassaro, B., Vasques, A.C., Geloneze, B., et al. (2020). Interleukin-17 acts in the hypothalamus reducing food intake. Brain Behav. Immun. 87, 272–285. https://doi.org/10.1016/j.bbi.2019.12.012.

13. Chen, J., Zhong, H., Yu, H., Sun, J., Shen, B., Xu, X., Huang, S., Huang, P., and Zhong, Y. (2023). Interleukin-17A modulates retinal inflammation by regulating microglial activation via the p38 MAPK pathway in experimental glaucoma neuropathy. FASEB J. 37, e22945. https://doi.org/10.1096/fj.202202056RR.

14. Enamorado, M., Kulalert, W., Han, S.J., Rao, I., Delaleu, J., Link, V.M., Yong, D., Smelkinson, M., Gil, L., Nakajima, S., et al. (2023). Immunity to the microbiota promotes sensory neuron regeneration. Cell 186, 607–620.e17. https://doi.org/10.1016/j.cell.2022.12.037.

15. Balthasar, N., Coppari, R., McMinn, J., Liu, S.M., Lee, C.E., Tang, V., Kenny, C.D., McGovern, R.A., Chua, S.C., Jr., Elmquist, J.K., and Lowell, B.B. (2004). Leptin receptor signaling in POMC neurons is required for normal body weight homeostasis. Neuron 42, 983–991. https://doi.org/10.1016/j.neuron.2004.06.004.

16. Li, H., Xu, Y., Jiang, Y., Jiang, Z., Otiz-Guzman, J., Morrill, J.C., Cai, J., Mao, Z., Xu, Y., Arenkiel, B.R., et al. (2023). The melanocortin action is biased toward protection from weight loss in mice. Nat. Commun. 14, 2200. https://doi.org/10.1038/s41467-023-37912-z.

17. Ma, Y., Murgia, N., Liu, Y., Li, Z., Sirakawin, C., Konovalov, R., Kovzel, N., Xu, Y., Kang, X., Tiwari, A., et al. (2022). Neuronal miR-29a protects from obesity in adult mice. Mol. Metab. 61, 101507. https://doi.org/10.1016/j.molmet.2022.101507.

18. González-García, I., García-Clavé, E., Cebrian-Serrano, A., Le Thuc, O., Contreras, R.E., Xu, Y., Gruber, T., Schriever, S.C., Legutko, B., Lintelmann, J., et al. (2023). Estradiol regulates leptin sensitivity to control feeding via hypothalamic Cited1. Cell Metab 35, 438–455.e7. https://doi.org/10.1016/j.cmet.2023.02.004.

19. El Malki, K., Karbach, S.H., Huppert, J., Zayoud, M., Reissig, S., Schüler, R., Nikolaev, A., Karram, K., Münzel, T., Kuhlmann, C.R.W., et al. (2013). An alternative pathway of imiquimod-induced psoriasis-like skin inflammation in the absence of interleukin-17 receptor a signaling. J. Invest. Dermatol. 133, 441–451. https://doi.org/10.1038/jid.2012.318.

20. Yu, H., Rubinstein, M., and Low, M.J. (2022). Developmental single-cell transcriptomics of hypothalamic POMC neurons reveal the genetic trajectories of multiple neuropeptidergic phenotypes. Elife 11, e72883. https://doi.org/10.7554/eLife.72883.

21. Shuai, K., and Liu, B. (2003). Regulation of JAK–STAT signalling in the immune system. Nat. Rev. Immunol. 3, 900–911. https://doi.org/10.1038/nri1226.

22. Carow, B., and Rottenberg, M.E. (2014). SOCS3, a Major Regulator of Infection and Inflammation. Front. Immunol. 5, 58. https://doi.org/10.3389/fimmu.2014.00058.

23. Abdelaal, M., le Roux, C.W., and Docherty, N.G. (2017). Morbidity and mortality

associated with obesity. Ann. Transl. Med. *5*, 161. https://doi.org/10.21037/atm.2017.03.107.

24. Mori, H., Hanada, R., Hanada, T., Aki, D., Mashima, R., Nishinakamura, H., Torisu, T., Chien, K.R., Yasukawa, H., and Yoshimura, A. (2004). Socs3 deficiency in the brain elevates leptin sensitivity and confers resistance to diet-induced obesity. Nat. Med. *10*, 739–743. https://doi.org/10.1038/nm1071.

25. Reed, A.S., Unger, E.K., Olofsson, L.E., Piper, M.L., Myers, M.G., Jr., and Xu, A.W. (2010). Functional Role of Suppressor of Cytokine Signaling 3 Upregulation in Hypothalamic Leptin Resistance and Long-Term Energy Homeostasis. Diabetes *59*, 894–906. https://doi.org/10.2337/db09-1024.

26. Wang, Z., do Carmo, J.M., da Silva, A.A., Bailey, K.C., Aberdein, N., Moak, S.P., and Hall, J.E. (2019). Role of SOCS3 in POMC neurons in metabolic and cardiovascular regulation. Am. J. Physiol. Regul. Integr. Comp. Physiol. *316*, R338–R351. https://doi.org/10.1152/ajpregu.00163.2018.

27. Kievit, P., Howard, J.K., Badman, M.K., Balthasar, N., Coppari, R., Mori, H., Lee, C.E., Elmquist, J.K., Yoshimura, A., and Flier, J.S. (2006). Enhanced leptin sensitivity and improved glucose homeostasis in mice lacking suppressor of cytokine signaling-3 in POMC-expressing cells. Cell Metab. *4*, 123–132. https://doi.org/10.1016/j.cmet.2006.06.010.

28. Padilla, S.L., Reef, D., and Zeltser, L.M. (2012). Defining POMC neurons using transgenic reagents: impact of transient Pomc expression in diverse immature neuronal populations. Endocrinology *153*, 1219–1231. https://doi.org/10.1210/en.2011-1665.

29. Yasukawa, H., Ohishi, M., Mori, H., Murakami, M., Chinen, T., Aki, D., Hanada, T., Takeda, K., Akira, S., Hoshijima, M., et al. (2003). IL-6 induces an anti-inflammatory response in the absence of SOCS3 in macrophages. Nat. Immunol. *4*, 551–556. https://doi.org/10.1038/ni938.

30. Bouret, S.G., Bates, S.H., Chen, S., Myers, M.G., Jr., and Simerly, R.B. (2012). Distinct roles for specific leptin receptor signals in the development of hypothalamic feeding circuits. J. Neurosci. *32*, 1244–1252. https://doi.org/10.1523/jneurosci.2277-11.2012.

31. Xu, A.W., Kaelin, C.B., Takeda, K., Akira, S., Schwartz, M.W., and Barsh, G.S. (2005). PI3K integrates the action of insulin and leptin on hypothalamic neurons. J. Clin. Invest. *115*, 951–958. https://doi.org/10.1172/jci24301.

32. Berglund, E.D., Liu, C., Sohn, J.W., Liu, T., Kim, M.H., Lee, C.E., Vianna, C.R., Williams, K.W., Xu, Y., and Elmquist, J.K. (2013). Serotonin 2C receptors in pro-opiomelanocortin neurons regulate energy and glucose homeostasis. J. Clin. Invest. *123*, 5061–5070. https://doi.org/10.1172/jci70338.

33. Lee, C.H., Song, D.K., Park, C.B., Choi, J., Kang, G.M., Shin, S.H., Kwon, I., Park, S., Kim, S., Kim, J.Y., et al. (2020). Primary cilia mediate early life programming of adiposity through lysosomal regulation in the developing mouse hypothalamus. Nat. Commun. *11*, 5772. https://doi.org/10.1038/s41467-020-19638-4.

34. Ryding, A.D., Sharp, M.G., and Mullins, J.J. (2001). Conditional transgenic technologies. J. Endocrinol. *171*, 1–14. https://doi.org/10.1677/joe.0.1710001.

35. Shao, X., Somlo, S., and Igarashi, P. (2002). Epithelial-specific Cre/lox recombination in the developing kidney and genitourinary tract. J. Am. Soc. Nephrol. *13*, 1837–1846. https://doi.org/10.1097/01.asn.0000016444.90348.50.

36. Kilkenny, C., Browne, W.J., Cuthill, I.C., Emerson, M., and Altman, D.G. (2010). Improving bioscience research reporting: the ARRIVE guidelines for reporting animal research. PLoS Biol. *8*, e1000412. https://doi.org/10.1371/journal.pbio.1000412.

37. Garrido, A., Kim, E., Teijeiro, A., Sánchez Sánchez, P., Gallo, R., Nair, A., Matamala Montoya, M., Perna, C., Vicent, G.P., Muñoz, J., et al. (2022). Histone acetylation of bile acid transporter genes plays a critical role in cirrhosis. J. Hepatol. *76*, 850–861. https://doi.org/10.1016/j.jhep.2021.12.019.

38. Chaves-Perez, A., Santos-de-Frutos, K., de la Rosa, S., Herranz-Montoya, I., Perna, C., and Djouder, N. (2022). Transit-amplifying cells control R-spondins in the mouse crypt to modulate intestinal stem cell proliferation. J. Exp. Med. *219*, e20212405. https://doi.org/10.1084/jem.20212405.

39. Gomes, A.L., Teijeiro, A., Burén, S., Tummala, K.S., Yilmaz, M., Waisman, A., Theurillat, J.P., Perna, C., and Djouder, N. (2016). Metabolic Inflammation-Associated IL-17A Causes Non-alcoholic Steatohepatitis and Hepatocellular Carcinoma. Cancer Cell *30*, 161–175. https://doi.org/10.1016/j.ccell.2016.05.020.

40. Bosso, G., Cipressa, F., Moroni, M.L., Pennisi, R., Albanesi, J., Brandi, V., Cugusi, S., Renda, F., Ciapponi, L., Polticelli, F., et al. (2019). NBS1 interacts with HP1 to ensure genome integrity. Cell Death Dis. *10*, 951. https://doi.org/10.1038/s41419-019-2185-x.

41. Berman, J.W., and Basch, R.S. (1980). Amplification of the biotin-avidin immunofluorescence technique. J. Immunol. Methods *36*, 335–338. https://doi.org/10.1016/0022-1759(80)90138-6.

42. Bosso, G., Cipressa, F., Tullo, L., and Cenci, G. (2023). Co-amplification of CBX3 with EGFR or RAC1 in human cancers corroborated by a conserved genetic interaction among the genes. Cell Death Discov. *9*, 317. https://doi.org/10.1038/s41420-023-01598-5.

43. Kumar, K., Oli, A., Hallikeri, K., Shilpasree, A.S., and Goni, M. (2022). An optimized protocol for total RNA isolation from archived formalin-fixed paraffin-embedded tissues to identify the long non-coding RNA in oral squamous cell carcinomas. MethodsX *9*, 101602. https://doi.org/10.1016/j.mex.2021.101602.

44. Piñeiro-Hermida, S., Bosso, G., Sánchez-Vázquez, R., Martínez, P., and Blasco, M.A. (2023). Telomerase deficiency and dysfunctional telomeres in the lung tumor microenvironment impair tumor progression in NSCLC mouse models and patient-derived xenografts. Cell Death Differ. *30*, 1585–1600. https://doi.org/10.1038/s41418-023-01149-6.

45. Zhan, C., Zhou, J., Feng, Q., Zhang, J.E., Lin, S., Bao, J., Wu, P., and Luo, M. (2013). Acute and long-term suppression of feeding behavior by POMC neurons in the brainstem and hypothalamus, respectively. J. Neurosci. *33*, 3624–3632. https://doi.org/10.1523/jneurosci.2742-12.2013.

STAR★METHODS

KEY RESOURCES TABLE

REAGENT or RESOURCE	SOURCE	IDENTIFIER
Antibodies		
Anti-goat Alexa Fluor 488	Invitrogen	Cat# A11055; RRID: AB_2534102
Anti-streptavidin Alexa Fluor 555	AAT Bioquest	Cat#16989; RRID: N/A
Anti-POMC	Sigma Aldrich	Cat# SAB2500826; RRID: AB_10605136
Anti-SOCS3	Proteintech	Cat# 66797-1-Ig; RRID: AB_2882141
Anti-IL17RA	Santa Cruz	Cat# sc-376374; RRID: AB_10991331
Anti-IL-17A	Invitrogen	Cat# PA5-79470; RRID: AB_2746586
Chemicals, peptides, and recombinant proteins		
DAPI	Sigma	D9542
Mowiol 4-88	Sigma	81381
BSA	Merck	A7906
Chow diet	Teklad	2918
HFD 45%	Brogaarden	D12451
TRIzol	Sigma	15596026
Critical commercial assays		
Vectastain ABC HRP Kit (Peroxidase, Mouse IgG)	Vector Laboratories	PK-4002
Avidin-biotin blocking kit	Palex	416430
M-MLV Reverse Transcriptase	Thermofisher	28025013
GoTaq SYBR Green Master Mix	Promega	A6002
Mouse: *Pomc-Cre*	Balthasar et al.,[15]	MGI: 3640616
Mouse: *Il17ra*(flox-flox)	El Malki et al.,[19]	MGI:5498882
Mouse: *Socs3*(flox-flox)	Yasukawa et al.,[29]	MGI:3051525
Oligonucleotides		
Primers for Genotyping	This Paper Table S1	N/A
Primers for RT-qPCR		
Software and algorithms		
GraphPad Prism 9.4.0	GraphPad Software	https://www.graphpad.com/scientific-software/prism/
Illustrator 26.3.1	Adobe	https://.adobe.com/products/illustrator.html
Image J 53c software	NIH	https://imagej.nih.gov/ij/
Photoshop 23.4.0	Adobe	https://adobe.com/products/photoshop.html
R Statistical Package V4.0.3 and R Studio		https://www.r-studio.com/
Other		
Fluorescence confocal microscopy	Leica	TCS SP5 MP

RESOURCE AVAILABILITY

Lead contact

Further information and requests for resources and reagents should be directed to and will be fulfilled by the lead contact, Nabil Djouder (ndjouder@cnio.es). The sharing of materials described in this work could be subject to standard material transfer agreements.

Materials availability

This study did not generate unique reagents.

Data and code availability

- This study did not generate any datasets. All data reported in this paper will be shared by the lead contact upon request.
- This paper does not report original code.
- Any additional information required to reanalyze the data reported in this paper is available from the lead contact upon request.

EXPERIMENTAL MODEL AND STUDY PARTICIPANT DETAILS

Animal models

Il17ra$^{(\Delta/\Delta)Pomc}$ and *Socs3*$^{(\Delta/\Delta)Pomc}$ mice were generated in our lab by crossing *Pomc-Cre*[15] (MGI: 3640616) mice with *Il17ra*$^{(flox-flox)}$ [19] (MGI:5498882) and *Socs3*$^{(flox-flox)}$ [29] (MGI:3051525) mice, respectively. More precisely, matings were conducted between *Pomc-Cre* mice heterozygous for the Cre allele and heterozygous for the floxed allele (+/flox). Littermate controls from the same cohort and strain of mice were always used in this study.

Only 8 week-old males were used for the study. All experiments were approved by the CNIO-ISCIII (Instituto de Salud Carlos III) Ethics Committee, Institutional Animal Care and Use Committee (IACUC), the Ethical Committee for animal experimentation (CEIyBA) (PROEX 172/18; PROEX 173.3/22) and Community of Madrid (CAM) and performed in accordance with the guidelines for ethical conduct in the care and use of animals as stated in the international guiding principles for biomedical research involving animals developed by the Council for International Organizations of Medical Sciences and as described in the ARRIVE guidelines.[36]

METHOD DETAILS

Mouse conditions and housing

All mice have been housed at the animal facility of the Spanish National research Centre (CNIO) in pathogen-free conditions, with a 12-h light–dark cycle between 8:00 and 20:00 in a temperature-controlled room (23 $\pm$ 1°C) following the recommendations of the EUMORPHIA Consortium for animal housing, unless stated otherwise. All mice have been backcrossed to C57BL/6 for at least seven generations.

Mouse diets

Mice were fed either a ND (18% fat, 58% carbohydrates and 24% proteins) (Harlan Laboratories, 2018S) or a HFD (45% fat, 35% carbohydrates and 20% proteins) (Research Diets, D12451). Food and water were provided *ad libitum.*

Mouse genotyping

The genotyping was performed as previously reported[1,37–39] using the following couples of primers:

Cre-Fw: 5′-CCATCTGCCACCAGCCAG-3′
Cre-Rv: 5′-TCGCCATCTTCCAGCAGG-3′
Cre control Fw: 5′- ACTGGGATCTTCGAACTCTTTGGAC-3′
Cre control Rv: 5′- GATGTTGGGGCACTGCTCATTCACC-3′
Socs3 Fw: 5′-GCGGGCAGGGGAAGAGACTGTCTGGGGTTG-3′
Socs3 Rv1: 5′-GGCGCACGGAGCCAGCGTGGATCTGCG-3′
Socs3 Rv2: 5′-AGTCCGCTTGTCAAAGGTATTGTCCCAC-3′
Il17ra Fw: 5′- GGCAGCCTTTGGGATCCCAAC-3′
Il17ra Rv: 5′-CTACTCTTCTCACCAGCGCGC-3′

Body weight

Mouse body weight has been measured weekly beginning at 8 weeks by using an analytical balance as previously described.[1]

Tissue preparation

Freshly collected tissues were fixed in 10% buffered formalin solution overnight and embedded in paraffin and processed as previously reported.[1,37,38,40] Mice were euthanized using CO_2 chambers. Tissues were quickly removed from mice and weighted using an analytical balance. For molecular analysis, the tissues were washed in PBS and frozen at -80.

Immunofluorescence

Avidin-biotin immunofluorescence technique has been performed as previously described.[41] Briefly, tissue sections of 3 μm were deparaffinized, rehydrated and antigen retrieved by using 1 M sodium citrate buffer (pH 6.5). After blocking endogenous peroxidase using 3% H_2O_2 for 10 min, and permeabilized in 0.5% Triton X-100 in PBS for 1 hour, sections were blocked for 1 hr at room temperature with avidin-biotin blocking kit diluted in 5% BSA dissolved in PBS 1X. Furthermore, sections were incubated with primary antibodies (anti-POMC, anti-IL17R, anti-SOCS3 and anti-IL17A) overnight at 4°C using the following concentrations. Then, the sections were incubated with biotinylated secondary

antibodies (1:200) diluted in PBS/ 5% BSA solution for 1h at RT, followed by the incubation with streptavidin-HRP (1:200) diluted in PBS/ 5% BSA solution for 30 min at RT.

Eventually, the sections were incubated with secondary antibodies anti-goat AF488 (1:500) and anti-streptavidin AF555 (1:500) and DAPI for 1 hour at RT. The pictures were acquired with confocal microscope and quantified with Image J software.

Reverse transcription-quantitative polymerase chain reaction (RT-qPCR)

Total RNA was extracted from frozen tissue, using TRIzol as previously reported[42] or extracted from paraffin-embedded tissue as previously described.[43] The cDNA was synthesized with M-MLV reverse transcriptase and GoTaq Real-Time was used to carry out RT-qPCRs.[44] Ct values of each gene were normalized to Ct value of *18s* and $2^{-\Delta\Delta Ct}$ was calculated. Finally, the fold changes of each gene were obtained normalizing the value of different groups to the control samples of the experiment. RT-qPCR primers are listed in Table S1.

Bioinformatics analysis

Publicly available RNA sequencing technology single-cell sequencing and trap-sequencing datasets from neurons https://cellxgene.cziscience.com/ and precisely POMC-expressing neurons GSE153753, GSE181539 [2,20] were used to analyze *Il17a*, *Il17ra*, *Pomc*, and *Rorc* genetic expression profiles. The average of the normalized count values (base mean) from the different datasets were used to represent the genetic expression.

QUANTIFICATION AND STATISTICAL ANALYSIS

Image analysis and quantifications

To quantify the immunofluorescence staining, 5 images per slide from each mouse were obtained. Single or double positive cells located anatomically near the ventral part of the third ventricle, specifically within the arcuate nucleus (ARC), were counted and normalized to the total number of DAPI-positive cells in the same ARC region, as indicated above. Data are represented as percentages and were calculated using the formula: (number of DAPI-positive cells in the arcuate nucleus / 100) x number of positive cells, as previously reported.[2,45] All quantifications were performed manually in a blind manner. Each dot in the graphs represents data from an individual mouse.

Statistical analysis

Statistical analyses were performed using GraphPad PrismV8.3.0 software. Statistical significance (*p* value) (*$p \leq 0.05$; **$p \leq 0.01$; ***$p \leq 0.001$) between the means of two groups was determined using unpaired two-tailed Student's *t* test or two-way ANOVA. Results are expressed as the mean value $\pm$ s.e.m. *n* represents the number of mice used in each experiment.